九州大学学術情報リポジトリ
Kyushu University Institutional Repository

Simultaneous Arsenic and Iron Oxidation for One-Step Scorodite Crystallization Using Mn Oxide

Nishi, Ryohei
Department of Earth Resources Engineering, Faculty of Engineering, Kyushu University

Kitjanukit, Santisak
Department of Earth Resources Engineering, Faculty of Engineering, Kyushu University

Kondo, Taiki
Department of Earth Resources Engineering, Faculty of Engineering, Kyushu University

Okibe, Naoko
Department of Earth Resources Engineering, Faculty of Engineering, Kyushu University

https://hdl.handle.net/2324/4737403

出版情報：Materials Transactions. 62 (12), pp.1791-1797, 2021-12-01. 日本金属学会
バージョン：
権利関係：©2021 The Japan Institute of Metals and Materials

KYUSHU UNIVERSITY

Materials Transactions, Vol. 62, No. 12 (2021) pp. 1791 to 1797
©2021 The Japan Institute of Metals and Materials

Simultaneous Arsenic and Iron Oxidation for One-Step Scorodite Crystallization Using Mn Oxide

Ryohei Nishi, Santisak Kitjanukit, Taiki Kondo and Naoko Okibe*

Department of Earth Resource Engineering, Faculty of Engineering, Kyushu University, Fukuoka 819-0395, Japan

The necessity of arsenic (As) removal from metallurgical wastewaters is increasing. Despite its wide recognition as a natural oxidant, the utility of Mn oxide for scorodite production is mostly unknown. In acidic solutions containing both As(III) and Fe^{2+}, simultaneous oxidation of the two progressed by MnO_2 and the resultant As(V) and Fe^{3+} triggered the formation of crystalline scorodite ($FeAsO_4{\cdot}2H_2O$). At 0.5% or 0.25% MnO_2, 98% or 91% As was immobilized by day 8. The resultant scorodite was sufficiently stable according to the TCLP test, compared to the regulatory level in US and Chile (5 mg/L): 0.11 ± 0.01 mg/L at 0.5% MnO_2, 0.78 ± 0.05 mg/L at 0.25% MnO_2. For the oxidation of As(III) and Fe^{2+}, 54% (at 0.5% MnO_2) or 14% (at 0.25% MnO_2) of initially added MnO_2 remained undissolved and the rest dissolved in the post As(III) treatment solution. For the Mn recycling purpose, the combination of Mn^{2+}-oxidizing bacteria and biogenic birnessite (as homogeneous seed crystal) was used to recover up to 99% of dissolved Mn^{2+} as biogenic birnessite ($(Na,Ca)0.5(Mn^{IV},Mn^{III})_2O_4{\cdot}1.5H_2O$), which can be utilized for the oxidation treatment of more dilute As(III) solutions at neutral pH. Although further optimization is necessary, the overall finding in this study indicated that Mn oxide could be utilized as a recyclable oxidant source for different As(III) treatment systems.
[doi:10.2320/matertrans.MT-M2021120]

(Received June 22, 2021; Accepted September 15, 2021; Published October 22, 2021)

Keywords: *arsenite, As(III)-oxidation, scorodite, Mn oxide, Mn recycle, birnessite, Mn-oxidizing bacteria*

1. Introduction

Arsenic (As)-contaminated wastewaters are a growing problem in metallurgical industries to secure future copper supply from As-bearing minerals such as enargite (Cu_3AsS_4) and tennantite ($Cu_{12}As_4S_{13}$). Generally, the treatment of highly toxic As(III) requires its pre-oxidation to less mobile/toxic As(V), followed by the As immobilization step.[1,2] Removing soluble As as scorodite mineral ($Fe^{III}As^{V}O_4{\cdot}2H_2O$) is regarded as an optimal approach for As disposal due to its high stability and density.[3] In earlier studies, high concentrations of As(V) (~hundreds of millimolar) have been chemically mineralized into scorodite by hydrothermal or atmospheric treatments at temperatures mostly 95–160°C.[3–8] After such treatments, some residual As remain to be treated in the form of As(V), as well as As(III) that had persisted in the pre-oxidation step. There are also some occasions wherein more dilute As(III) solutions (~25 mM) are produced.[8] In order to enable scorodite mineralization at such thermodynamically less feasible, lower As concentrations even under milder conditions, microbiological approaches have also been proposed.[8–14]

Manganese (Mn) is the 10th most abundant element in the Earth's crust and 2nd (only to iron) most common heavy metal.[15] Over 30 Mn oxyhydroxide minerals are known in diverse geological settings, which are thought to participate in various chemical reactions to affect groundwater and soil compositions.[15] In nature, such Mn oxides can behave as chemical oxidants, consequently playing a critical role in the geochemistry of various heavy metals (e.g., Cr(III),[16] Co^{2+},[17] As(III),[18–21] Fe^{2+}[22]). The more electro-positive standard redox potential of the $Mn(IV)/Mn^{2+}$ couple (+1.3 V) than that of As(V)/As(III) (+0.56 V) enables the oxidation of As(III) by MnO_2, as described by eq. (1):

$$H_3As^{III}O_3 + Mn^{IV}O_2 + H^+ \rightharpoonup H_2As^{V}O_4^- + Mn^{2+} + H_2O \quad (1)$$

This reaction involves the formation of Mn(III) intermediate ($Mn^{III}OOH^*$) (eq. (2)), which can be later reduced to Mn^{2+} by further reacting with As(III) (eq. (3)):[23]

$$H_3As^{III}O_3 + 2Mn^{IV}O_2 + H_2O \rightharpoonup H_2As^{V}O_4^- + 2Mn^{III}OOH^* + H^+ \quad (2)$$

$$H_3As^{III}O_3 + 2Mn^{III}OOH^* + 3H^+ \rightharpoonup H_2As^{V}O_4^- + 2Mn^{2+} + 3H_2O \quad (3)$$

The standard redox potential of the $Mn(IV)/Mn^{2+}$ is also more electro-positive than that of Fe^{3+}/Fe^{2+} (+0.77 V; pH 2.0), thus Mn oxides are capable of oxidizing Fe^{2+} to Fe^{3+} as described by eq. (4):[19]

$$2Fe^{2+} + Mn^{IV}O_2 + 4H^+ \rightharpoonup 2Fe^{3+} + Mn^{2+} + 2H_2O \quad (4)$$

The oxidation behavior of Mn oxides was also studied under the coexistence of As(III) and Fe^{2+}.[24–27] Han *et al.*[24] reported that the presence of Fe^{2+} significantly inhibits the removal (oxidation and sorption) of As(III) by MnO_2 in acidic conditions at 25°C. This was attributed to the formation of Fe(III) compounds passivating the MnO_2 surface. The authors speculated the formation of poorly crystalline particles of FeOHAs and $FeAsO_4$.[24] Likewise, Ehlert *et al.*[25] reported that the oxidation of Fe^{2+} by birnessite proceeds significantly faster than that of As(III) and the resultant Fe^{3+} precipitates as As-sequestering ferrihydrite at circumneutral pH and 25°C.[25] The As(III) oxidation kinetics by a poorly crystalline hexagonal birnessite at different Fe^{2+} concentrations was studied by Wu *et al.*[26,27] at pH 6. The authors reported the competitive oxidation of Fe^{2+} over As(III) and suggested that the resultant precipitation of Fe(III)-(hydr)oxides on the birnessite surface plays an important role in As(III) oxidation and As sequestration.

Nonetheless, no study so far reported the production of crystalline scorodite by utilizing the oxidation ability of Mn

---

*Corresponding author, E-mail: okibe@mine.kyushu-u.ac.jp

oxides. According to eq. (1)–(4), Mn^{2+} is reductively dissolved from Mn oxide upon oxidation of As(III) and Fe^{2+}. The metal value of dissolved Mn^{2+} should be ideally recovered from the post As(III) treatment reaction. Regenerating Mn oxide from Mn^{2+} in the post As(III) treatment solution would enable Mn recycling in this regard. One of the most economically feasible approaches for Mn oxide regeneration would be the use of Mn-oxidizing microorganisms since microbial Mn oxidation proceeds at neutral pH (instead of alkali pH in chemical reactions). For this aim, the objectives of this study were set to evaluate; (i) the utility of Mn oxide for the oxidative removal of As(III) as scorodite, and (ii) the feasibility of Mn recovery from the post As(III) treatment solution using the Mn-oxidizing bacterium.

2. Materials and Methods

2.1 Effect of MnO_2 on individual oxidation of As(III) and Fe^{2+}

Different doses of MnO_2 (138-09675, Wako chemicals; 0.15, 0.25 or 0.5% (w/v)) was added into 100 mL deionized water ($pH_{initial}$ 1.5 with H_2SO_4) containing either 1000 mg/L (13 mM) of As(III) (added as $NaAsO_2$) or 1000 mg/L (18 mM) of Fe^{2+} (added as $FeSO_4 \cdot 7H_2O$) in 300 mL Erlenmeyer flasks. The flasks were incubated shaken at 100 rpm, 70°C. Samples were regularly withdrawn to monitor pH, Eh (vs. SHE) and concentrations of Fe^{2+} (*o*-phenanthroline method[28)]), As(III) (molybdenum blue method[29,30)]) and total soluble Fe, As and Mn (ICP-OES; Optima8300, PerkinElmer). All tests were done in duplicate flasks.

2.2 Effect of MnO_2 on simultaneous oxidation of As(III) and Fe^{2+} for scorodite precipitation

Different doses of MnO_2 (0.15, 0.25 or 0.5% (w/v)) were added into 200 mL deionized water ($pH_{initial}$ 1.5 with H_2SO_4) containing both 1000 mg/L As(III) and 1000 mg/L Fe^{2+} (to set the Fe/As molar ratio at 1.3) in 500 mL Erlenmeyer flasks. The flasks were incubated shaken at 100 rpm, 70°C. Sampling and analytical methods were described in section 2.1. All tests were done in duplicate flasks.

2.3 Toxicity characteristic leaching procedure (TCLP) test

In order to examine the stability of scorodite crystals formed in section 2.2., the TCLP test was performed according to the EPA method 1311 (US EPA method 1311). An aliquot of scorodite sample (0.15 g) was added into 5 mL serum bottles containing 3 mL acetate buffer (pH 4.9). Serum bottles were rotated at 30 rpm, 25°C, for 18 hours using a rotary shaker. The leachate was filtered (0.6 μm) and measured for the total soluble Fe and As concentrations (ICP-OES). The test was conducted in duplicate bottles.

2.4 Mn recycling via microbiological Mn oxide (birnessite) regeneration

2.4.1 Microorganism

Mn-oxidizing bacterium, *Pseudomonas* sp. SK3 (isolated from a metal-refinery wastewater treatment system[25)]) was used. Its routine sub-culturing used half-strength lysogeny broth (LB) medium (0.5% (w/v) NaCl; 0.5% (w/v) tryptone; 0.25% (w/v) yeast extract) in Erlenmeyer flasks (shaken at 120 rpm, 25°C). Cells were pre-grown overnight, collected and washed with 0.8% (w/v) NaCl solution prior to use in the following Mn oxidation tests.

2.4.2 Regeneration of Mn-oxide from the post As(III)-treatment solution

The post As(III)-treatment solution after scorodite precipitation (section 2.2) was subjected to the following Mn recycling step by utilizing the microbial Mn-oxidizing activity. Pre-grown *Pseudomonas* sp. SK3 cells (10^9 cells/mL) were inoculated into 100 ml of the post As(III)-treatment solution (diluted by 16-fold) supplemented with inorganic salts (2 mM $MgSO_4 \cdot 7H_2O$; 0.07 mM $CaCl_2 \cdot 2H_2O$; 3 μM $CuCl_2$) and organic substrates (0.01% (w/v) yeast extract; 0.01% (w/v) peptone; 1 mM glucose). The initial pH was adjusted to 5.0 or 7.0 with NaOH. The effect of seed crystals was also compared by feeding 0.1% (w/v) biogenic birnessite. Biogenic birnessite was separately produced by *Pseudomonas* sp. SK3, collected, freeze-dried prior to use (the freeze-drying process deactivated bacterial cells). Flasks were incubated shaken at 120 rpm at 25°C. Samples were regularly taken to monitor pH and the total soluble Mn concentration (ICP-OES). All tests were done in duplicate flasks.

2.5 X-ray diffraction (XRD) and scanning electron microscope (SEM) analyses

Mn precipitates formed in section 2.4.2 were collected by filtration (0.45 μm), washed with deionized water and freeze-dried overnight prior to the XRD (UltimaIV, Rigaku; CuKα 40 mA, 40 kV) analysis and SEM (VE-9800, KEYENCE) observation.

3. Results and Discussion

3.1 Individual oxidation of As(III) and Fe^{2+} by MnO_2

As(III) oxidation at different MnO_2 doses is shown in Fig. 1. pH remained unchanged throughout the experiment (data not shown). Since the total soluble As concentration was nearly unchanged throughout the test (data not shown), both As(III) and As(V) ions remained mostly soluble without noticeable adsorption or precipitation on the MnO_2 surface. As(III) was readily oxidized to As(V) by MnO_2 with an increasing reaction speed at higher MnO_2 doses (Fig. 1(a)). Accordingly, Mn^{2+} was released via reductive dissolution of MnO_2 (Fig. 1(a)). At 0.25% and 0.5% MnO_2, the reaction proceeded with a molar ratio of Δ[As(III) oxidized]/Δ[Mn dissolved] at around 1 (Fig. 1(b)), according to eq. (1). At a lower MnO_2 dose of 0.15%, however, the molar ratio decreased towards the later stage (Fig. 1(b)), possibly caused by the increasing passivation effect of the MnO_2 surface with Mn(III) intermediate.[23)]

Likewise, the Fe^{2+} oxidation trend by different doses of MnO_2 is shown in Fig. 2. The total soluble Fe concentration remained unchanged throughout the test (data not shown). Therefore, Fe^{2+} oxidized to Fe^{3+} by MnO_2 existed in the form of a soluble ion. The Fe^{2+} oxidation reaction was seen as a distinctive two-phase process, where the reaction

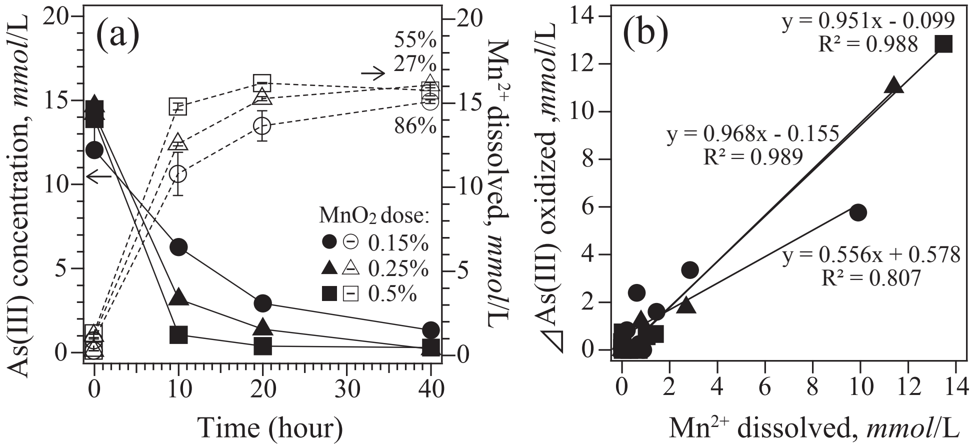

Fig. 1 The effect of MnO_2 as an oxidant for As(III) in acidic solutions ($pH_{initial}$ 1.5). Different MnO_2 doses (●○ 0.15%; ▲△ 0.25%; ■□ 0.5%) were compared: (a) The oxidation trend of 13 mM As(III) by MnO_2 (solid symbols) and the resultant reductive dissolution of Mn^{2+} (open symbols). At 40 hours, 86%, 55% or 27% of MnO_2 was reductively dissolved at 0.15, 0.25 or 0.5% MnO_2 doses, respectively. (b) Correlation between the amount of As(III) oxidized versus Mn^{2+} reductively dissolved.

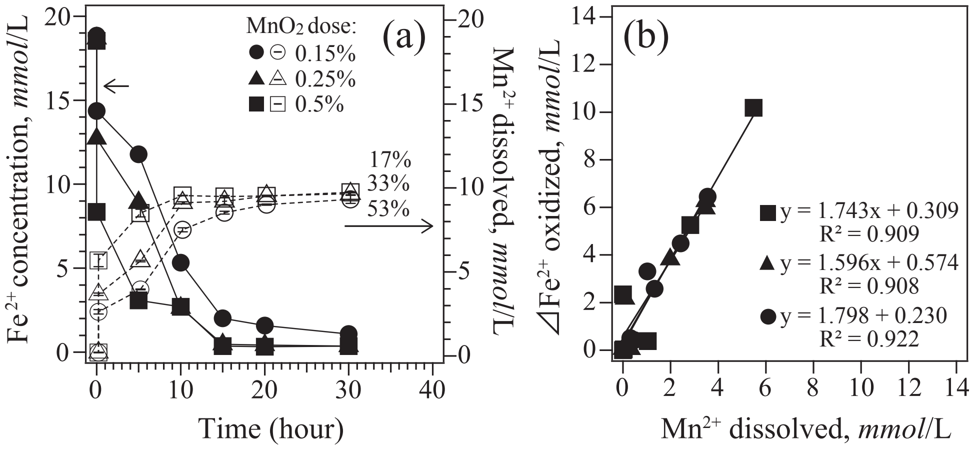

Fig. 2 The effect of MnO_2 as an oxidant for Fe^{2+} in acidic solutions ($pH_{initial}$ 1.5). Different MnO_2 doses (●○ 0.15%; ▲△ 0.25%; ■□ 0.5%) were compared: (a) The oxidation trend of 18 mM Fe^{2+} by MnO_2 (solid symbols) and the resultant reductive dissolution of Mn^{2+} (open symbols). At 30 hours, 53%, 33% or 17% of MnO_2 was reductively dissolved at 0.15, 0.25 or 0.5% MnO_2 doses, respectively. (b) Correlation between the amount of Fe^{2+} oxidized versus Mn^{2+} reductively dissolved.

proceeds instantly upon contact with MnO_2 (accounting for 23–55% Fe^{2+} oxidation) in the first phase, followed by the second slower reaction phase (Fig. 2(a)). This phenomenon was also observed by Wu *et al.*,[26] wherein passivation of Fe(III)-hydroxides on the MnO_2 surface were thought to be the cause (more likely amorphous jarosite, $KFe_3(SO_4)_2(OH)_6$, under the highly acidic condition in this study, while not evidenced by XRD). Stoichiometrically, one mole of Mn(IV) reacts with 2 moles of Fe^{2+} according to eq. (4). The results shown in Fig. 2(b) are consistent with this theoretical calculation.

3.2 Simultaneous oxidation of As(III) and Fe^{2+} by MnO_2 and the subsequent scorodite precipitation

In acidic solutions containing both As(III) and Fe^{2+}, oxidation of As(III) nearly completed by day 4 at 0.5% MnO_2 (As(III) 0.1 mM), and by day 8 at 0.25% MnO_2 (As(III) 0.4 mM) (Fig. 3(a)). pH remained unchanged throughout the experiment (data not shown). The oxidation of Fe^{2+} progressed more rapidly than As(III) and was mostly completed by day 2 ($Fe^{2+} < 0.6$ mM; Fig. 3(b)) at both MnO_2 doses. When a smaller MnO_2 dose (0.15%) was used, the oxidation of As(III) and Fe^{2+} nearly plateaued after day 3 at the halfway point (data not shown). The resultant production of As(V) and Fe^{3+} triggered the formation of As(V)–Fe^{3+} precipitates: Immobilization of Fe (Fig. 3(b)) proceeded more rapidly than that of As (Fig. 3(a)), causing the transition of the molar ratio of [Fe precipitated] to [As precipitated] (Fe_{ppt}/As_{ppt}) shifting from 2.2 to 1.3–1.5 during the reaction (Fig. 3(d)). Upon the oxidation of As(III) and Fe^{2+}, MnO_2 was reductively dissolved to release Mn^{2+} (24 mM or 26 mM at 0.25% or 0.5% MnO_2, respectively; Fig. 3(c)), according to the stoichiometry based on eq. (1) and eq. (4).

The color of As(V)–Fe^{3+} precipitates turned from brown to pale-green at day 4, indicating the transition of amorphous precursors to scorodite crystals via SO_4^{2-}-mediated phase transformation.[12] The precipitates were identified as crystalline scorodite by XRD at both 0.25% and 0.5% MnO_2 (Fig. 4(c), (d)), while the final product remained amorphous at a lower MnO_2 dose of 0.15% (Fig. 4(b)). Through this 2-stage scorodite crystallization process,[12] 98% As was

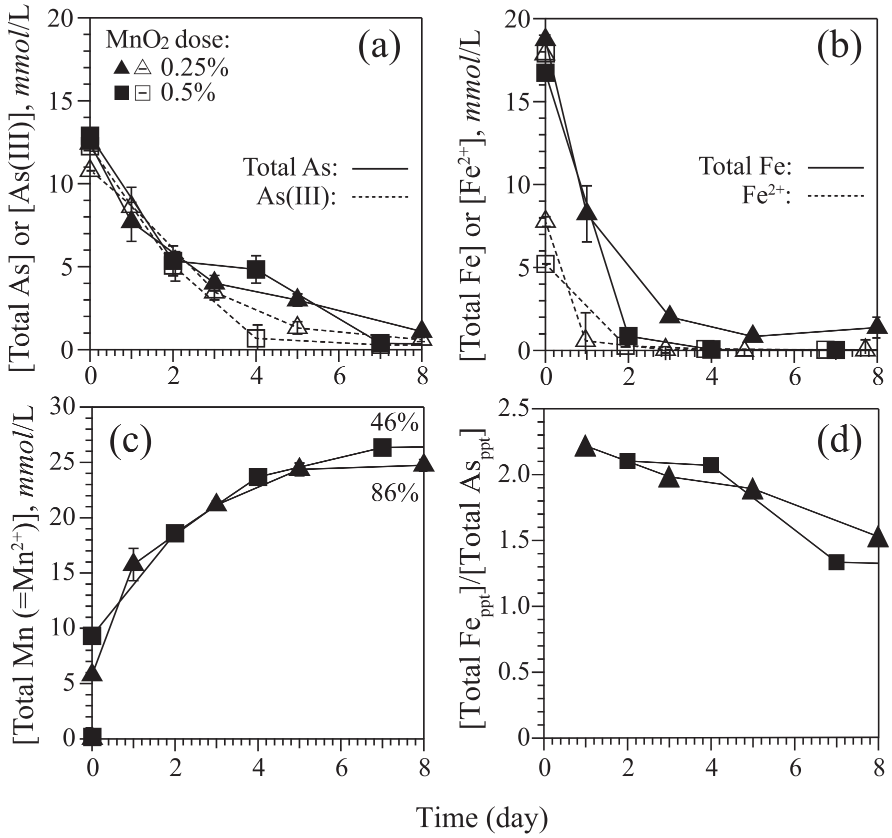

Fig. 3 Simultaneous oxidation of As(III) and Fe^{2+} by MnO_2 and their subsequent precipitation. The effect of different initial MnO_2 doses (▲△ 0.25%, ■□ 0.5%) was compared: (a) Changes in the concentration of total soluble As (solid symbols) or As(III) (open symbols). (b) Changes in the concentration of total soluble Fe (solid symbols) or Fe^{2+} (open symbols). (c) Mn^{2+} released into the solution via reductive dissolution of MnO_2. On day 8, 86% or 46% of MnO_2 was reductively dissolved at 0.25 or 0.5% MnO_2, respectively. (d) The transition of the molar ratio of [Total Fe precipitated] to [Total As precipitated] (Fe_{ppt}/As_{ppt}). The molar ratios were calculated from the concentrations of total soluble As (a) and Fe (b).

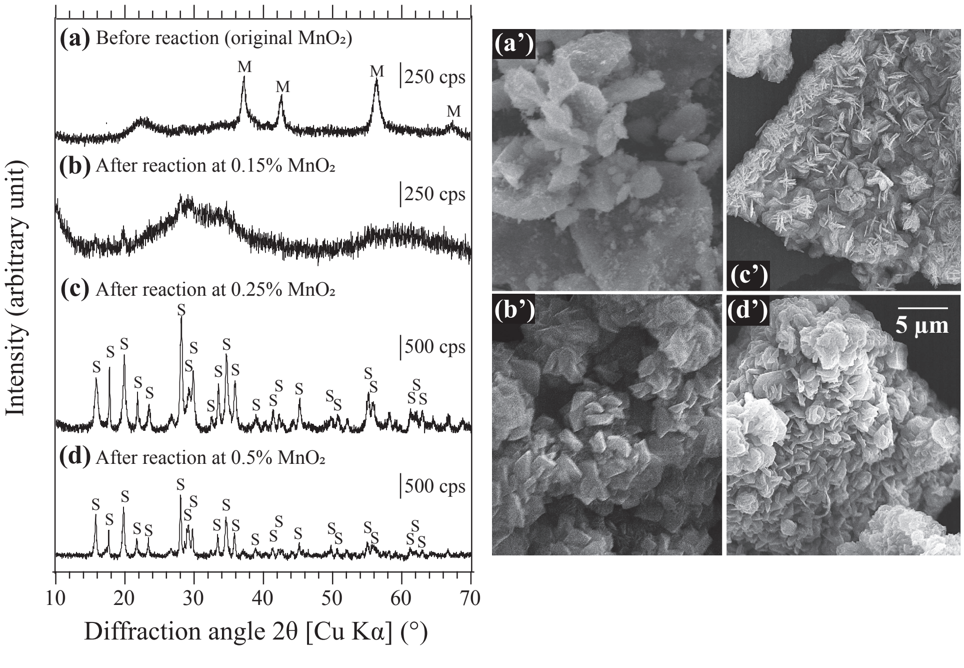

Fig. 4 XRD patterns and SEM images before (a, a′) and after (b–d, b′–d′) the scorodite precipitation reaction at different MnO_2 doses: 0.15% (b, b′), 0.25% (c, c′), 0.5% (d, d′). XRD peaks: M (ε-MnO_2; Akhtenskite, PDF No. 01-089-5171), S (scorodite; JCPDS 37-0468).

eventually immobilized using 0.5% MnO_2, and 91% As immobilized using 0.25% MnO_2 by day 8 (Fig. 3(a)). SEM images show the formation of scorodite crystals with a distinctive needle-like morphology (Fig. 4(c′), (d′)), compared to the surface of original MnO_2 surface (Fig. 4(a′)) and amorphous precipitates (Fig. 4(b′)).

The stability of As(V)–Fe^{3+} precipitates was evaluated by the TCLP test (Fig. 5). A negligible amount of Fe was leached in all tests, indicating the re-precipitation of Fe^{3+} at pH 4.9.[8] Immobilizing As as amorphous ferric arsenate (using 0.15% MnO_2) was shown to be unpractical due to its high leachability (As leached; 8.12 ± 0.26 mg/L) which is higher than the regulatory level in US and Chile (5 mg/L). The amount of As leached from crystalline scorodite was slightly different between at 0.25% (0.78 ± 0.05 mg/L) and 0.5% MnO_2 (0.11 ± 0.01 mg/L) (Fig. 5), but sufficiently low compared to most of the chemically synthesized scorodite (As leached; 0.1–13.6 mg/L).[5,6,31] Based on the amount of Mn^{2+} dissolved upon the oxidation of As(III) and Fe^{2+} (Fig. 3(c)), it can be calculated that 54% (0.5% MnO_2) or 14% (0.25% MnO_2) of initially added MnO_2 remained undissolved after the reaction, as a mixture with the As(V)–Fe^{3+} precipitates.

3.3 Regeneration of Mn-oxide from the post As(III) treatment water

After the oxidative removal of As(III) as scorodite, Mn^{2+} ions reductively dissolved from MnO_2 remained in the solution. With an attempt to recover the metal value of Mn from the post As(III) treatment solution, the following Mn oxide regeneration test was conducted using the Mn-oxidizing bacterium. After the scorodite precipitation reaction using 0.25% MnO_2 in Fig. 3 (day 8), the remaining solution containing 0.4 mM As(III), 0.6 mM As(V) and 24 mM Mn^{2+} was collected and diluted by 16-folds to 0.03 mM As(III), 0.04 mM As(V) and 1.5 mM Mn^{2+}. Regeneration of Mn oxide by *Pseudomonas* sp. SK3 cells only, sterile biogenic birnessite only, or the combination of the two is compared in Fig. 6.

The XRD peaks of Mn precipitates recovered at 140 hours (Fig. 6) were compared in Fig. 7.

Naturally occurring Mn oxides (often poorly crystalline) found in circumneutral pH environments are likely to be of a microbiological origin.[32] Bacterial Mn^{2+} oxidation is typically catalyzed by multicopper oxidase enzymes via two-step one-electron transfer reaction ($Mn^{2+} \rightharpoonup Mn(III) \rightharpoonup Mn(IV)$),[32] and can be represented as eq. (5), so as the chemical Mn^{2+} oxidation reaction at alkaline pH. Biogenic birnessite, formerly written as $(Na, Ca)0.5(Mn^{IV}, Mn^{III})_2O_4\cdot 1.5H_2O$, is known to be formed by *Pseudomonas* sp. SK3 in this reaction.[33]

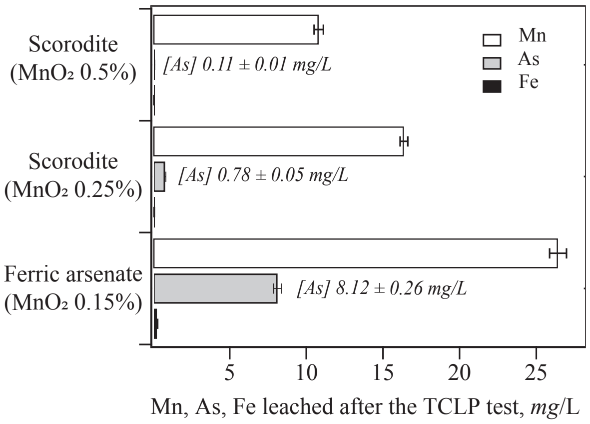

Fig. 5 The TCLP test result (As, Fe and Mn) of As(V)–Fe^{3+} precipitates produced by using 0.5% MnO_2 (crystalline scorodite), 0.25% MnO_2 (crystalline scorodite) and 0.15% MnO_2 (amorphous ferric arsenate). As(V)–Fe^{3+} precipitates were collected as a mixture with residual undissolved MnO_2.

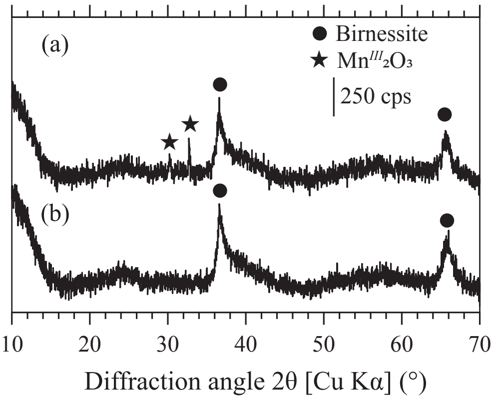

Fig. 7 XRD peaks of Mn precipitates collected at 140 hours (in Fig. 6). (a) Mn precipitates formed by birnessite seeds only. (b) Mn precipitates formed by the synergistic effect of *Pseudomonas* sp. SK3 cells plus birnessite seeds.

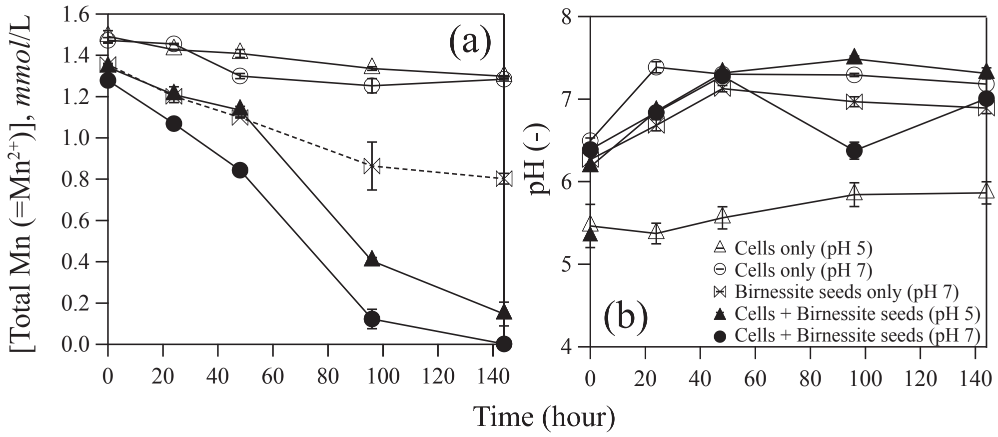

Fig. 6 Microbiological recovery of dissolved Mn^{2+} from the post As(III) treatment water. Changes in the total soluble Mn concentration (a) and pH (b) are shown. For the oxidative precipitation of Mn^{2+}, either *Pseudomonas* sp. SK3 cells only (△ $pH_{initial}$ 5.0; ○ $pH_{initial}$ 7.0), biogenic birnessite seeds only (▷◁ $pH_{initial}$ 7.0) or the combination of the two (▲ $pH_{initial}$ 5.0; ● $pH_{initial}$ 7.0) were compared.

$$\mathrm{Mn}^{2+} + 1/2\ \mathrm{O}_2 + \mathrm{H}_2\mathrm{O} \rightharpoonup \mathrm{Mn}^{IV}\mathrm{O}_2 + 2\mathrm{H}^+ \qquad (5)$$

As shown in Fig. 6, *Pseudomonas* sp. SK3 cells only were ineffective in oxidizing 1.6 mM Mn^{2+}, likely due to the presence of residual As in the solution. In the absence of toxic As species, *Pseudomonas* sp. SK3 cells were able to complete the oxidation of this amount of Mn^{2+}.33)

Biogenic birnessite itself could lead to autocatalytic, chemical Mn^{2+} oxidation by the comproportionation of Mn^{2+} and MnO_2, especially in alkaline conditions (eq. (6)).32,34,35)

$$\mathrm{Mn}^{2+} + \mathrm{Mn}^{IV}\mathrm{O}_2 + \mathrm{H}_2\mathrm{O} \rightarrow \mathrm{Mn}^{III}{}_2\mathrm{O}_3 + 2\mathrm{H}^+ \qquad (6)$$

To see the possible synergistic effect of bacterial Mn^{2+} oxidation (eq. (5)) and autocatalytic chemical Mn^{2+} oxidation (eq. (6)), biogenic birnessite only or *Pseudomonas* sp. SK3 plus biogenic birnessite was also tested. In addition to its effect as a chemical Mn^{2+}-oxidizing agent (eq. (6)), birnessite can also act as the solid surface for bacterial cell attachment and seed crystals for further birnessite formation.

The use of 0.1% birnessite only was more effective than cells only but was still incapable of completing the Mn oxidation (43% Mn recovery; Fig. 6): Although 0.1% birnessite should theoretically oxidize and precipitate all Mn^{2+} present, secondary mineral passivation of $Mn^{III}{}_2O_3$ (Fig. 7(a)) on the birnessite surface significantly slowed down the reaction. The combination of the two (cells and birnessite), on the other hand, showed a synergistic effect, and the Mn^{2+} oxidation was promoted (Fig. 6). The birnessite particles could have provided solid support for SK3 cell attachment, enabling the cells to be less affected by the As toxicity and retain Mn^{2+}-oxidizing activity. Fresh birnessite formed by SK3 cells could have further oxidized the remaining Mn^{2+}, thus promoting the synergistic effect. Due to its poor crystallinity, some amorphous birnessite was dissolved when $pH_{initial}$ 5.0 was used, consequently pushing up the pH to neutral (Fig. 6(b)). At $pH_{initial}$ 7.0, the Mn^{2+} oxidation was the most effective and was completed by 140 hours.

Mn oxide regenerated from the post As(III) treatment solution was poorly crystalline birnessite and it was not feasible to reuse it as the oxidant for further scorodite production under the highly acidic pH (Okibe, unpublished data). However, our separate study demonstrated that such "bioactive" birnessite (birnessite minerals retaining active Mn-oxidizing bacterial cells) could be effectively utilized as the column carrier for the continuous oxidation treatment system for more dilute As(III) solutions under neutral pH.36)

Studies are ongoing further to acclimate Mn-oxidizing bacteria to As(III). Also, our separate studies indicate that optimization of chemical/microbial synergistic effect could allow higher Mn^{2+} load upon regeneration of Mn-oxide (Okibe, unpublished data). This Mn recycle step could be made more robust upon such further improvement.

4. Conclusion

As(III) was readily oxidized to As(V) by MnO_2 with a molar ratio of Δ[As(III) oxidized]/Δ[Mn dissolved] at around 1. Fe^{2+} was oxidized to Fe^{3+} by MnO_2 with a molar ratio of $\Delta[Fe^{2+}$ oxidized]/Δ[Mn dissolved] at around 2 ($pH_{initial}$ 1.5). In acidic solutions containing both ions, simultaneous oxidation of As(III) and Fe^{2+} was observed, and the resultant As(V) and Fe^{3+} triggered the formation of crystalline scorodite (98% As immobilized at 0.5% MnO_2 and 91% As at 0.25% MnO_2 by day 8). Scorodite was sufficiently stable based on the TCLP test (0.11 ± 0.01 mg/L at 0.5% MnO_2, 0.78 ± 0.05 mg/L at 0.25% MnO_2), compared to the regulatory level in US and Chile (5 mg/L). Upon the oxidation of As(III) and Fe^{2+}, 54% (at 0.5% MnO_2) or 14% (at 0.25% MnO_2) of initially added MnO_2 remained undissolved after the reaction. It was possible to recycle dissolved Mn^{2+} from the post As(III) treatment solution via microbiological Mn oxide regeneration as amorphous birnessite, which could be of use in the oxidation treatment of more dilute As(III) solutions at neutral pH.

Acknowledgment

S.K is grateful for the financial assistance provided by the Kyushu University Advanced Graduated Program in Global Strategy for Green Asia.

REFERENCES

1) W.R. Cullen and K.J. Reimer: Chem. Rev. **89** (1989) 713–764.
2) D. Lievremont, P.N. Bertin and M.C. Lett: Biochimie **91** (2009) 1229–1237.
3) P.A. Riveros, J.E. Dutrizac and P. Spencer: Can. Metall. Quart. **40** (2001) 395–420.
4) A.J. Monhemius and P.M. Swash: JOM **51** (1999) 30–33.
5) S. Singhania, Q. Wang, D. Filippou and G.P. Demopoulos: Metall. Mater. Trans. B **37** (2006) 189–197.
6) T. Fujita, R. Taguchi, H. Kubo, E. Shibata and T. Nakamura: Mater. Trans. **50** (2009) 321–331.
7) A. Iizuka, K. Shinoda and E. Shibata: Mater. Trans. **59** (2018) 843–849.
8) M. Tanaka and N. Okibe: Minerals **8** (2018) 23.
9) P. Gonzalez-Contreras, J. Weijma and C.J.N. Buisman: Cryst. Growth Des. **12** (2012) 2699–2706.
10) N. Okibe, M. Koga, S. Morishita, M. Tanaka, S. Heguri, S. Asano, K. Sasaki and T. Hirajima: Hydrometallurgy **143** (2014) 34–41.
11) N. Okibe, S. Morishita, M. Tanaka, K. Sasaki, T. Hirajima, K. Hatano and A. Ohata: Hydrometallurgy **168** (2017) 121–126.
12) M. Tanaka, N. Okibe and K. Sasaki: Hydrometallurgy **180** (2018) 144–152.
13) N. Okibe and Y. Fukano: Biotechnol. Lett. **41** (2019) 1403–1413.
14) N. Okibe, R. Nishi, Y. Era and T. Sugiyama: Mater. Trans. **61** (2020) 387–395.
15) J.E. Post: Proc. Natl. Acad. Sci. USA **96** (1999) 3447–3454.
16) S.E. Fendorf and R.J. Zasoski: Environ. Sci. Technol. **26** (1992) 79–85.
17) A. Manceau, V.A. Drits, E. Silvester, C. Bartoli and B. Lanson: Am. Mineral. **82** (1997) 1150–1175.
18) J.K. Yang, M.O. Barnett, J. Zhuang, S.E. Fendorf and P.M. Jardine: Environ. Sci. Technol. **39** (2005) 7102–7110.
19) M.J. Scott and J.J. Morgan: Environ. Sci. Technol. **29** (1995) 1898–1905.
20) J.N. Moore, J.R. Walker and T.H. Hayes: Clays Clay Miner. **38** (1990) 549–555.
21) C. Tournassat, L. Charlet, D. Bosbach and A. Manceau: Environ. Sci. Technol. **36** (2002) 493–500.
22) D.F.A. Koch: Aust. J. Chem. **10** (1957) 150–159.
23) B.J. Lafferty, M. Ginder-Vogel and D.L. Sparks: Environ. Sci. Technol. **44** (2010) 8460–8466.
24) X. Han, Y.L. Li and J.D. Gu: Geochim. Cosmochim. Acta **75** (2011) 368–379.
25) K. Ehlert, C. Mikutta and R. Kretzschmar: Environ. Sci. Technol. **48** (2014) 11320–11329.

26) Y. Wu, W. Li and D.L. Sparks: J. Colloid Interface Sci. **457** (2015) 319–328.
27) Y. Wu, R.K. Kukkadapu, K.J.T. Livi, W. Xu, W. Li and D.L. Sparks: ACS Earth Space Chem. **2** (2018) 256–268.
28) D.H. Caldwell and R.B. Adams: J. Am. Water Works Ass. **38** (1946) 727–730.
29) J. Murphy and J.P. Riley: Anal. Chim. Acta **27** (1962) 31–36.
30) S. Blomqvist, K. Hjellström and A. Sjösten: Int. J. Environ. Anal. Chem. **54** (1993) 31–43.
31) M.L. Caetano, V.S.T. Ciminelli, S.D.F. Rocha, M.C. Spitale and C.L. Caldeira: Hydrometallurgy **95** (2009) 44–52.
32) B.M. Tebo: Annu. Rev. Earth Planet. Sci. **32** (2004) 287–328.
33) S. Kitjanukit, K. Takamatsu and N. Okibe: Water **11** (2019) 507.
34) J.W. Murray, J.G. Dillard, R. Giovanoli, H. Moers and W. Stumm: Geochim. Cosmochim. Acta **49** (1985) 463–470.
35) T. Takashima, K. Hashimoto and R. Nakamura: J. Am. Chem. Soc. **134** (2012) 1519–1527.
36) R. Nishi, S. Kitjanukit, K. Nonaka and N. Okibe: Hydrometallurgy **196** (2020) 105416.